Critical exponents of four-dimensional random-field Ising systems

Alexander K. Hartmann*
Department of Physics, University of California, Santa Cruz CA 95064, USA and
Ecole Normale Supérieure
24, Rue Lhomond, 75231 Paris Cedex 05, France
(Dated: January 24, 2002)

The ferromagnet-to-paramagnet transition of the four-dimensional random-field Ising model with Gaussian distribution of the random fields is studied. Exact ground states of systems with sizes up to 32^4 are obtained using graph theoretical algorithms. The magnetization, the disconnected susceptibility, the susceptibility and a specific heat-like quantity are calculated. Using finite-size scaling techniques, the corresponding critical exponents are obtained: $\beta = 0.15(6)$, $\overline{\gamma} = 3.12(10)$, $\gamma = 1.57(10)$ and $\alpha = 0$ (logarithmic divergence). Furthermore, values for the critical randomness $h_c = 4.18(1)$ and the correlation-length exponent $\nu = 0.78(10)$ were found. These independently obtained exponents are compatible with all (hyper-) scaling relations and support the two-exponent scenario ($\overline{\gamma} = 2\gamma$).

I. INTRODUCTION

Phase transitions of pure systems[1,2] are already relatively well understood. The critical behavior of all physical quantities can be described via critical exponents. These exponents are related through (hyper-) scaling relations to each other, so that only *two* independent exponents remain. In contrast, phase transitions in systems with (quenched) disorder[3] exhibit many puzzles and are still far from being understood.

In theoretical physics, the random-field Ising magnet (RFIM) is a widely studied prototypical disordered system. It is believed[4,5] to be in the same universality class as the diluted antiferromagnet in a field, which can be studied experimentally[6].

For a while it was thought[7–9] that the critical behavior of the d-dimensional RFIM is equal to that of the $d-2$ pure ferromagnet. This would imply that the $d=3$ RFIM exhibits no ordered phase. This is not true, as has been shown later rigorously[10]. In the meantime, a scaling theory[11–13] for the RFIM was developed, where the dimension d has been replaced by $d-\theta$ in the hyperscaling relations, θ (sometimes called also y) being a *third* independent exponent, in contrast to the pure case. An alternative approach[14,15] leads to the consequence that θ is not independent but related to the exponent η describing the divergence of the (disconnected) susceptibility via $\theta = 2-\eta$. Further evidence for the existence of only two independent exponent was recently found by high-temperature expansions[16]. This was confirmed in three dimensions by Monte Carlo simulations[17] and by exact ground-state calculations[18,19]. But the exponents found in these works do not fulfill the scaling relation $\alpha + 2\beta + \gamma = 2$, being $\alpha, \beta, \gamma = \nu(2-\eta)$ the critical exponents for the specific heat, the magnetization and the susceptibility, respectively. On the other hand, the results obtained in a different way in the most thorough ground-state study in $d=3$ so far[20] indeed do not violate this scaling relation. Also, a modified scaling relation $\alpha + 2\beta + \gamma = 1$ was proposed[21], but the exponents obtained in Refs. 17–19 do not match the new relation either. Hence, to obtain more insight into the scaling behavior of the RFIM and to improve the knowledge of the critical behavior of random systems, here the four-dimensional model is studied.

The RFIM Hamiltonian is given by

$$\mathcal{H} = -J\sum_{\langle i,j\rangle} S_i S_j - \sum_i (h_i + H) S_i, \qquad (1)$$

where the $S_i = \pm 1$ are Ising spins, J is the interaction energy between nearest neighbors, $h_i \equiv h\epsilon_i$ is the random field and H an uniform external field. Here the case $H=0$ is studied, but small values of the external field are used to determine the susceptibility. The values ϵ_i are independently distributed according a Gaussian distribution with mean 0 and standard deviation 1, i.e. the probability distribution is

$$P(h_i) = \frac{1}{\sqrt{2\pi}\,h} \exp\left(-\frac{h_i^2}{2}\right). \qquad (2)$$

Hence, $h_i = h\epsilon_i$ is Gaussian distributed with standard deviation h. We shall consider finite-dimensional lattices with periodic boundary condition and $N = L^d$ spins. The results presented below are for $d=4$.

The canonical phase diagram in zero external field ($H=0$) of the RFIM in higher than two dimensions is shown in Fig. 1. For low temperatures and small randomness, the ferromagnetic couplings dominate, hence the system exhibits a long-range order. For higher temperatures, where the entropy dominates, or for higher random fields, where the spins are predominately aligned parallel to its local random fields, the system is paramagnetic.

For random-field distributions which exhibit a maximum at $h=0$, such as present in the Gaussian case, in mean-field theory[22] the phase transition is second order along the whole phase boundary. Furthermore, the renormalization group flow along the phase boundary approaches the $h=h_c$, $T=0$ fixed point[4], i.e. it controls the critical behavior. Therefore it can be expected

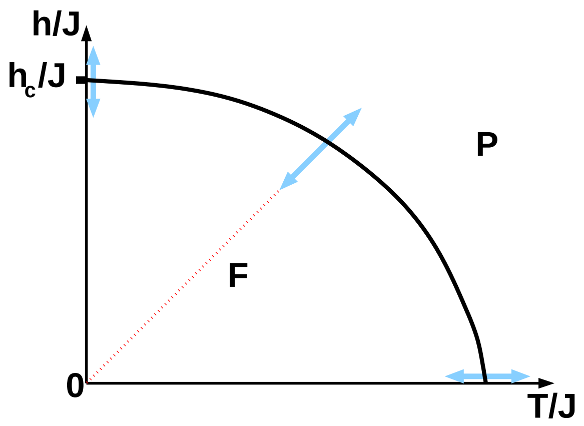

FIG. 1: A sketch of the phase boundary of the random field Ising model. The ferromagnetic phase is denoted by "F" and the paramagnetic phase by "P". The critical value of the random field at $T = 0$ is denoted by h_c. The lines with arrows at both ends indicate the path followed by varying J for some fixed value of h and T.

that the critical behavior along the whole phase boundary is equal to that at $h = h_c, T = 0$, and all critical exponents can be obtained from the zero temperature behavior. Working at $T = 0$ has the advantage that exact ground states of the RFIM can be calculated using modern graph theoretical algorithms in polynomial time[23–26]. This avoids equilibration problems often encountered in Monte Carlo simulations and, even better, allows to study much larger system sizes than before.

The $T = 0$ behavior of the four-dimensional RFIM has been studied[27] using exact ground states up to size $L = 10$. In addition to the random critical random field h_c, the exponents ν describing the divergence of the correlation length ξ and β for the magnetization were obtained. In this work, not only much larger systems sizes up to $N = 32^4$ are considered, but also the critical exponents α for the specific heat[19], γ for the susceptibility and $\overline{\gamma}$ for the disconnected susceptibility are obtained *independently*, i.e. without using scaling relations. This in turn allows to test (hyper-) scaling relations and to investigate the assumptions of two or three independent critical exponents. The main results of this paper are that the specific heat diverges logarithmically or maybe faster and that the two independent exponent scenario is supported.

The rest of the paper is organized as follows. Next, the algorithms used to calculated exact ground states are briefly explained. In the main section all observables and results are presented. In the final section the scaling relations are checked, the results discussed and a summary given.

II. ALGORITHMS

To calculate the exact ground states at given randomness h and field H, algorithms[23–26] from graph theory[28–30] were applied. To implement them, some algorithms from the LEDA library[31] were utilized.

Here the methods are just outlined. More details can be found in the literature cited below or in the pedagogical presentation in Ref. 26. For each realization of the disorder, given by the external field H and the values $\{h_i\}$ of the random fields, the calculation works by transforming the system into a network[32], calculating the maximum flow in polynomial time[33–37] and finally obtaining the spin configuration $\{S_i\}$ from the values of the maximum flow in the network. The running time of the latest maximum-flow methods has a peak near the phase transition and diverges[38,39] there like $O(L^{d+1})$ The first results of applying these algorithms to random-field systems can be found in Ref. 40. In Ref. 18 these methods were applied to obtain the exponents for the magnetization, the disconnected susceptibility and the correlation length from ground-state calculations up to size $L = 80$. The most thorough study of the ground states of the 3d RFIM so far is presented in Ref. 20. Other exact ground-state calculation of the 3d model can be found in Refs. 21,41,42. These techniques have also already applied to small four-dimensional systems[27].

Since the algorithms work only with integer values for all parameters, a value of $J = 10000$ was chosen here, and all values were rounded to its nearest integer value. This discreteness is sufficient, as shown in Ref. 20. All results are quoted relative to J (or assuming $J \equiv 1$).

Note that in cases where the ground-state is degenerate[43] it is possible to calculate all the ground-states in one sweep[44], see also Refs. 45,46. For the RFIM with a Gaussian distribution of fields, the ground state is non-degenerate, except for a two-fold degeneracy at certain values of the randomness, where the ground state changes, so it is sufficient to calculate just one ground state.

III. RESULTS

In this work, exact ground states for system sizes $L = 4$ to $L = 32$ for different values of the randomness h and with 4 different values $H = 0, H_L, 2H_L, 4H_L$ (only $H = 0$ for $L = 32$) were calculated. Near the transitions, an average over the disorder with the number $N_{\rm samp}$ of samples ranging from 3200 ($L = 32$) up to 40000 ($L = 4$) was performed, less samples were used away from the critical point, since the fluctuations are small outside the critical region. For details, see Tab. I.

We first concentrate on the case $H = 0$. The simulations with $H > 0$ were done to obtain the susceptibility, see below.

As, already mentioned, when studying *one* single finite sample of the disorder $\{h\epsilon_i\}$ as a function of h,

L	N_{samp}	H_L
4	40000	0.025
6	20000	0.02
8	7100	0.012
12	8500	0.006
16	4000	0.003
24	10000	0.0015
32	3200	–

TABLE I: The maximum number of samples N_{samp} used, and sizes of smallest non-zero uniform field H_L, for each system size L. As discussed in the text, the number of samples used was larger in the vicinity of the peaks in the susceptibility and specific heat than elsewhere.

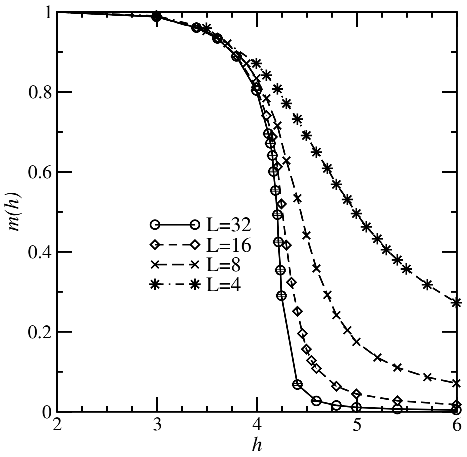

FIG. 2: Average magnetization as a function of random-field strength h. For clarity of the plot, only $L = 4, 8, 16, 32$ are shown. Error bars (shown for $L = 32$) are much smaller than symbol sizes. Lines are guides to the eyes only.

the ground state changes only at certain discrete values $h^{(1)}, h^{(2)}, \ldots, h^{M(\{\epsilon_i\})}$. Hence, quantities like the magnetization are stepwise constant as a function of h. This discreteness vanishes, when averaging over the disorder.

In Fig. 2 the average magnetization per spin

$$m \equiv [|M|]_h \equiv \left[\left|\frac{1}{N}\sum_i S_i\right|\right]_h \tag{3}$$

is shown as a function of the randomness h for system sizes $L = 4, 8, 16, 32$. The average over the disorder is denoted by $[\ldots]_h$, which is carried out (approximately) by repeating the calculation for N_{samp} independent realizations (samples) of the random fields $\{h\epsilon_i\}$. As expected, for small randomness the ground state is ferromagnetically ordered and disordered for large values of h. The curves become steeper with increasing h, indicating a phase transition near $h = 4.2$.

To study the transition more detailed, the Binder parameter[47,48]

$$g(L,h) \equiv \frac{1}{2}\left(3 - \frac{[\langle M^4\rangle]_h}{[\langle M^2\rangle]_h^2}\right) \tag{4}$$

is calculated, $\langle\ldots\rangle$ being the thermal disorder, (which is trivial at $T = 0$ if the ground state is non degenerate). The idea behind the definition of this quantity is that in the thermodynamic limit, the distribution of the order parameter should converge towards a delta function (with $g(L,h) = 1$) in the ordered phase and to a Gaussian distribution ($g(L,h = 0)$) in the disordered phase. The scaling theory for 2nd order phase transitions assumes, that the finite-size behavior is governed by the ratio L/ξ, ξ being the correlation length. At the critical point, where the correlation length is infinite, the parameters for different system sizes should intersect, since L/ξ is sero for all sizes L. In Fig. 3 the result for the 4d RFIM is shown, please note the enlarged scale.

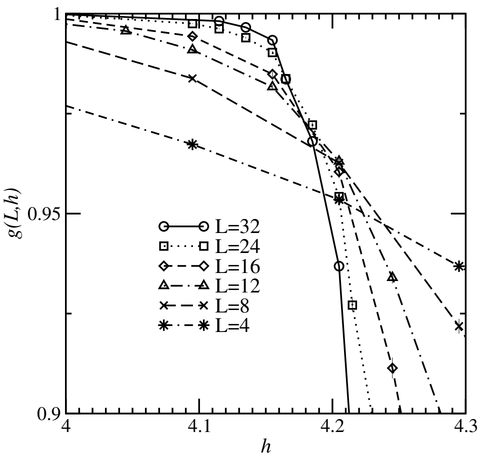

FIG. 3: Binder parameter $g(L,h)$ as a function of the randomness h for different system sizes L. For clarity of the plot, only $L = 6$ is omitted. Error bars are smaller than symbol sizes. Lines are guides to the eyes only.

Indeed all curves intersect near $h = 4.2$, compatible with the result for the magnetization. A systematic shift can be observed, which decreases with growing system size, and is due to finite-size effects in small systems. From the intersections of sizes $L \geq 8$, a value for the critical randomness of $h_c^{\mathrm{binder}} = 4.18(2)$ is estimated. Due to the finite-size effect observed here, small system sizes will be excluded from subsequents fits if they don't match the leading behavior.

To observe the specific heat singularity, here the bond energy E_J is studied[19], given by

$$E_J \equiv \frac{\partial F}{\partial J} = -\frac{1}{N}\sum_{\langle i,j\rangle}\langle S_i S_j\rangle, \tag{5}$$

where the sum is over nearest-neighbor pairs. E_J has an energy-like singularity in the vicinity of the phase boundary. Having differentiated *analytically* with respect to J, now $J = 1$ is set, and $T = 0$ considered only. A specific heat-like quantity is obtained by differentiating E_J *numerically* with respect to the random field h. A first-order finite difference is used to determine the derivative of E_J numerically and, since this is a more accurate representation of the derivative at the midpoint of the interval than at either endpoint, the "specific heat", C, at $T = 0$ is defined to be

$$C\left(\frac{h_1 + h_2}{2}\right) \equiv \frac{[E_J(h_1)]_h - [E_J(h_2)]_h}{h_1 - h_2}, \tag{6}$$

where h_1 and h_2 are two "close-by" values of h. A sufficiently fine mesh of random-field values is chosen such that the resulting data for C is smooth. Error bars are obtained by determining the "specific heat" from the corresponding finite difference as in Eq. (6) for each sample separately, and computing the standard deviation. The error bar is, as usual, the standard deviation divided by $\sqrt{N_{\rm samp} - 1}$.

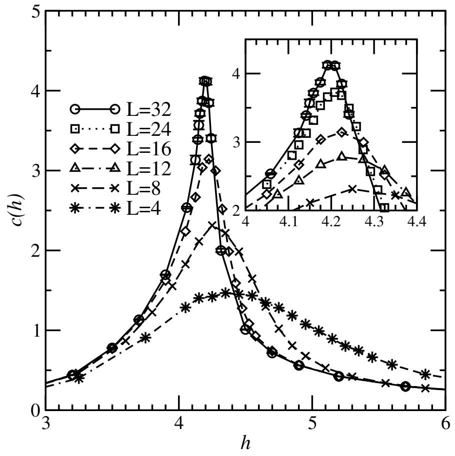

FIG. 4: Specific heat-like quantity $C = \partial^2 F/\partial h \partial J$ as a function of the randomness h for $L = 4, 8, 16, 32$. Error bars are only shown for $L = 32$. For the other system sizes the error bars are even smaller. The inset shows the region near the peaks enlarged for $L \geq 8$. Lines are guides to the eyes only.

In Fig. 4 the numerical results are exposed. The "specific heat" exhibits clear peaks, which grow in system size and move slightly left. The number of samples used is larger near the peak to compensate for the greater sample to sample fluctuations in this region.

In a finite system, finite-size scaling predicts for the singular part $C_{\rm s}$ of the specific heat

$$C_{\rm s} \sim L^{\alpha/\nu} \widetilde{C}\left((h - h_c)L^{1/\nu}\right), \tag{7}$$

where ν is the correlation length exponent. The "specific heat" peak will occur when the argument of the scaling function $\widetilde{C}$ takes some value, a_1 say, so the peak position $h^*(L)$ varies as

$$h^*(L) - h_c \approx a_1 L^{-1/\nu}, \tag{8}$$

and the value of the singular part of the "specific heat" at the peak varies as

$$C_{\rm s}^{\max}(L) \sim L^{\alpha/\nu}. \tag{9}$$

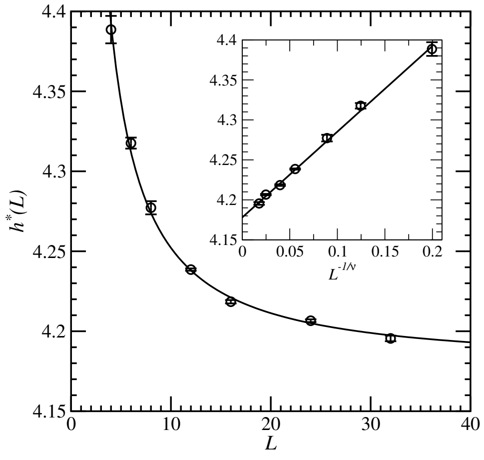

FIG. 5: A plot of the random field where the "specific heat" attains its maximum, as a function of system size L. The solid line shows a fit to the function $h^*(L) = h_c + a_1 L^{-1/\nu}$ with $h_c = 4.18$, $1/\nu = 0.78$, and $a_1 = 1.34$. The inset shows the data as a function of $L^{-1/\nu}$.

For each system size, parabolic fits were performed in the region of the peak to obtain $h^*(L)$ and the height of the peak, $C^{\max}(L)$. The shift of the maximum according to Eq. (8) can be used to estimate the infinite-size critical strength of the random field, h_c and the correlation-length exponent ν. The best fit gives

$$h_c = 4.182 \pm 0.006, \qquad 1/\nu = 1.28 \pm 0.14, \tag{10}$$

see Fig. 5. The probability Q was determined that the value of $\chi^2 = \sum_{i=1}^{N} (\frac{y_i - f(x_i)}{\sigma_i})^2$, with N data points $(x_i, y_i \pm \sigma_i)$ fitted to the function f, is worse than in the current fit[49] to quantify the quality of the fit. Here a value of $Q = 0.06$ was obtained , which is not very good. The reason is, that the error bars used for the positions and heights of the maxima were only the statistical error bars obtained from the fit of the parabolas, and which are often surprisingly small. Systematic errors, resulting from the fact that the peaks are in fact not parabolic, are not included in this way. Therefore, fits to a fourth order polynomials were tried, but the results turned out to be very unreliable and the fits very unstable against the change of the window over which the data was fitted. Hence, the parabolic fits were kept, were these effects were smaller, and the final value quoted is $h_c = 4.18(1)$.

Next, the singular behavior of C is determined by analyzing, how the peak value $C^{\max}$ scales with L. Please note[19] that at $T = 0$ the singular behavior C is equal to the singular behavior of $C' = -\partial^2 F/\partial h^2$, since $C = -C'h/J$ at $T = 0$.

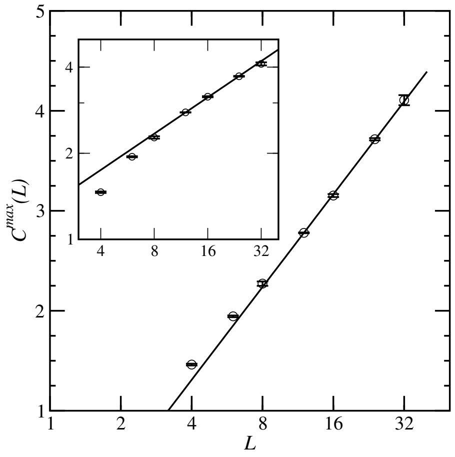

FIG. 6: The maximum $C^{\max}$ of the "specific heat" as a function of system size with logarithmically scaled L-axis. The lines shows the function $a + b \log L$ with $a = -0.53$ and $b = 1.33$. The inset shows the data in a double-logarithmic plot, the solid line being the function $a_2 L^{\alpha/\nu}$ with $\alpha/\nu = 0.419$ and $a_2 = 0.98$.

The first hypothesis is that the "specific heat" diverges logarithmically, as found in experiments for three-dimensional diluted antiferromagnets in a field[50]. Hence, the values of $C^{\max}$ are fitted ($L \geq 8$) to a function of the form

$$C^{\max}(L) = a + b \log L, \tag{11}$$

where the constant term a comes partly from the regular piece of the "specific heat". The quality $Q = 0.23$ of the fit is fair. In Fig. 6 the "specific heat" is shown in a logarithmic plot together with the fit function (11). For larger system sizes the datapoints follow very nicely a straight line, suggesting that C indeed may diverge logarithmically. Please note that the "specific heat" peaks seem to be rather symmetrical, which means that the amplitudes A_+, A_- (for $h > h_c\, h < h_c$) of C are almost equal. This is exactly what one expects in the case of a logarithmic divergence[51].

Also the possibility of a algebraic divergence was tested. For this purpose the data was fitted ($L \geq 8$) to the function

$$C^{\max}(L) = a_2 L^{\alpha/\nu}, \tag{12}$$

resulting in $\alpha/\nu = 0.419(9)$ and $a_2 = 0.98(2)$, the result is shown together with the data in a double logarithmic plot in the inset of Fig. 6. The quality $Q = 9 \times 10^{-3}$ of the fit is very bad. To check whether this is an effect of including too small system sizes into the fit, also a fit using only system sizes $L \geq 12$ was performed, resulting in $\alpha/\nu = 0.416(6)$, $a_2 = 0.99(1)$ and $Q = 0.16$ which is much better. Since for $L \geq 12$ the logarithmic fit has also a better quality $Q = 0.55$, and because the negative curvature in the double-logarithmic plot is more pronounced than a possible positive curvature in the single-logarithmic plot, still a logarithmic divergence seems more likely from this data, i.e.

$$\alpha = 0, \tag{13}$$

but an algebraic behavior with a small exponent cannot be excluded.

Next, the critical behavior of the magnetization is studied. The predictions from finite-size scaling is that near the critical point

$$m(h) = L^{-\beta/\nu} \tilde{m}((h - h_c) L^{1/\nu}). \tag{14}$$

This means, that by plotting $m(h)L^{\beta/\nu}$ against $L^{1/\nu}(h - h_c)$ with correct parameters h_c, ν and β/ν, the data points for different system sizes should collapse onto a single curve near $(h - h_c) = 0$. The values $h_c = 4.18$ and $1/\nu = 1.28$ from above were used. With

$$\beta/\nu = 0.17(5) \tag{15}$$

the best collapse of the data for $L \geq 8$ was obtained, which is presented in Fig. 7.

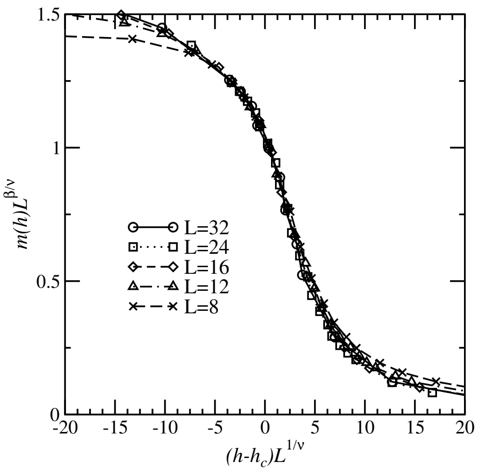

FIG. 7: Scaling plot of the rescaled absolute value $m(h)L^{\beta/\nu}$ magnetization as a function of of $(h - h_c)L^{1/\nu}$ with $h_c = 4.18$, $1/\nu = 1.28$ and $\beta/\nu = 0.17$. Error bars are smaller than symbol sizes. Lines are guides to the eyes only.

The singular behavior of the disconnected susceptibility

$$\chi_{\rm dis} \equiv L^d \left[M^2\right]_h \tag{16}$$

can be obtained in an analogous way to the magnetization. The following scaling behavior is assumed:

$$\chi_{\rm dis}(h) = L^{\overline{\gamma}/\nu} \tilde{\chi}_{\rm dis}((h - h_c) L^{1/\nu}). \tag{17}$$

From collapsing the date curves for $L \geq 8$, using $h_c = 4.18$ and $1/\nu = 1.28$, a value of

$$\overline{\gamma}/\nu = 3.63(0.05) \tag{18}$$

was found. The scaling plot is shown in Fig. 8. Please note that the scaling behavior of $h < h_c$ is worse than for $h > h_c$ (also, to a lesser extent, in Fig. 7). The reason is that for smaller fields the systems quickly become fully ordered ($m = 1$), i.e. scaling does not hold.

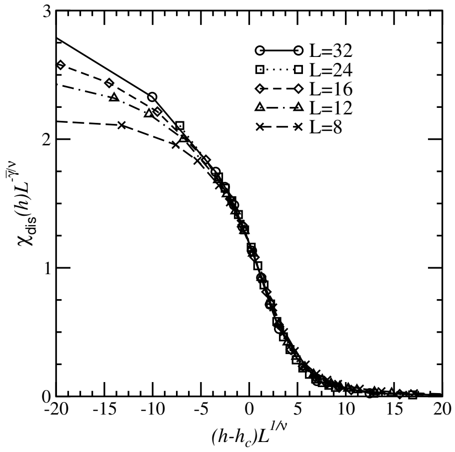

FIG. 8: Scaling plot of the rescaled disconnected susceptibility $\chi_{\rm dis}(h)L^{\overline{\gamma}/\nu}$ as a function of of $(h-h_c)L^{1/\nu}$ with $h_c = 4.18$, $1/\nu = 1.28$ and $\overline{\gamma}/\nu = 3.63$. Error bars are smaller than symbol sizes. Lines are guides to the eyes only.

Finally, the susceptibility and its related critical exponent γ is determined. This is done by considering the response to a small uniform external field $H > 0$. For each realization, the sign of H is chosen in the direction of the magnetization of the ground state. This prevents the whole system from flipping when applying a magnetic field to a system which is almost ferromagnetically ordered, which would mimic a false high susceptibility. The scaling behavior of the magnetization should not be affected by this choice.

The ground state for each realization and each value of h is calculated for $H_n = 0, H_L, 2H_L, 4H_L$. Near $H = 0$, the data points can be fitted very well with a parabola, the coefficient of the linear term gives the zero field susceptibility

$$\chi = dm/dH|_{H=0}. \tag{19}$$

To cope for the expected strong increase of χ with the system size, H_L must strongly decrease with L, in the order of the expected increase. For details see Ref. 19, the values of H_L are shown in Tab. I. Then, for each system size, a fit to a parabola through the four data points for the *average* magnetization $m(H_n)$ is performed. To estimate the error, a jackknife analysis[52] was used, in which the results for the magnetizations (for each system size and each strength of the disorder) is divided into K blocks, the average values calculated K times, each time omitting one of the blocks, and then K fits are performed. The error bar is estimated from the variance of the K results for the linear fitting parameter. Here

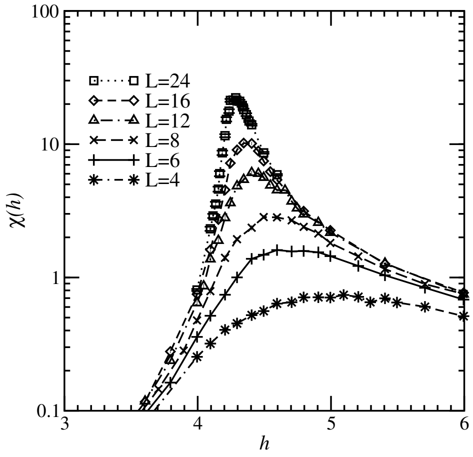

FIG. 9: Susceptibility χ as a function of the random-field strength h for system sizes $L = 4, 6, 8, 12, 16$, and 24. Error bars (shown for $L = 24$) are smaller than symbol sizes. Lines are guide to the eyes only.

$K = 50$ was used and checked that the result does not depend much on the choice of K.

The susceptibility χ as a function of h is presented in Fig. 9 for selected system sizes. It is seen that the height of the peak grows much faster than for the "specific heat". For the susceptibility, the following scaling behavior is expected:

$$\chi(h) = L^{\gamma/\nu}\tilde{\gamma}((h-h_c)L^{1/\nu}). \tag{20}$$

To analyze the divergence of χ, again parabolas were fitted to the data points near the peak to obtain the positions $h^*(L)$ and $\chi^{\max}(L)$ of the maximum. By fitting the data for $L \geq 8$ to a function $\chi^{\max}(L) = a_3 L^{\gamma/\nu}$, where γ describes the decay of the "connected" correlations at criticality, the following values were obtained ($Q = 0.54$)

$$\gamma/\nu = 1.82 \pm 0.01, \tag{21}$$

see Fig. 10.

It was also tried to fit the positions $H^*(L)$ of the maxima of the susceptibility to a scaling function of the from (8). But the quality of the fit was very bad ($Q < 10^{-7}$) for all ranges $[L_{\min}, 24]$ considered and the result for h_c was always too large ($h_c > 4.26 \pm 0.03$). This value is not only not compatible with the result from the "specific heat" C, but in clear contradiction to the Binder parameter (see Fig. 3). The reason is probably the stronger finite-size dependence of the position of the susceptibility peak in comparison to the position of the "specific heat" peak, please compare Figs. 4 and 9. Also, due to the four times higher numerical effort to determine χ, only simulations for $L \leq 24$ were performed. Furthermore, the peaks for the susceptibility are much broader than for the "specific heat", hence it is harder to determine the position of the peak precisely. Thus, the result $h_c = 4.18(1)$ from the previous measurement was kept.

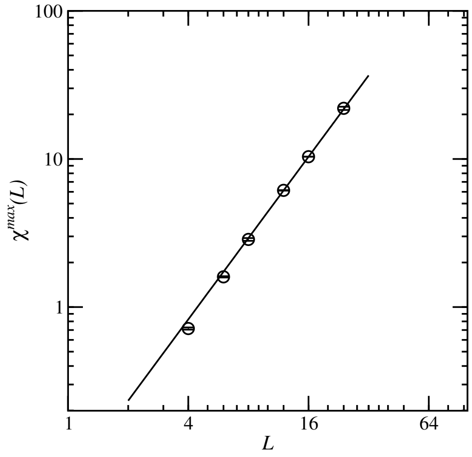

FIG. 10: The maximum $\chi^{\max}$ of the susceptibility as a function of system size L in a double logarithmic plot. The solid line represents a fit to the function $\chi^{\max}(L) = a_3 L^{\gamma/\nu}$, for sizes $L \geq 8$ yielding $\gamma/\nu = 1.82$ and $a_3 = 0.066$.

IV. DISCUSSION

Using graph-theoretical algorithms, exact ground states of random-field Ising systems were calculated in polynomial time. Using the LEDA library, system sizes up to $N = 32^4$ could be considered.

All critical exponents, describing the order-to-disorder transition at h_c were calculated independently. The following values, using $\gamma = \nu(2-\eta)$ and $\overline{\gamma} = \nu(4-\overline{\eta})$, for the values of the critical field h_c and the exponents were obtained:

$$\begin{array}{ll} h_c = 4.18 \pm 0.01, & \nu = 0.78 \pm 0.10 \\ \alpha = 0 & \beta = 0.13 \pm 0.05 \\ \eta = 0.18 \pm 0.01 & \overline{\eta} = 0.37 \pm 0.05 \\ \gamma = 1.42 \pm 0.20 & \overline{\gamma} = 2.83 \pm 0.50. \end{array} \quad (22)$$

Please note that the values for β, γ and $\overline{\gamma}$ carry a large error bar due to the uncertainty in the correlation-length exponent ν.

The results for the critical field, the correlation exponent and the exponent of the magnetization are compatible with values found formerly via the exact ground state calculations of small systems[27] up to $L = 10$, where $h_c = 4.17(5)$, $\beta = 0.13(2)$ and $\nu = 0.8(1)$ were obtained. The result for the susceptibility exponent is compatible with the result $\gamma = 1.45(5)$ which was found in a high-temperature expansion[16]. The results obtained here are also compatible with the exponents obtained recently[39] by the use of exact ground states as well but by evaluating mainly other quantities like distributions of domain-wall energies or fractal properties of domain walls. The main difference is that the results from Ref. 39 have a slight preference for the exponent α of the "specific heat" to be positive but small.

Next, the validity of the scaling relation for the "specific heat" is checked. For the Rushbrooke equality

$$\alpha + 2\beta + \gamma = 2 \quad (23)$$

one gets $\alpha + 2\beta + \gamma = 1.68(30)$, which is not very good but still within the error bars almost fulfilled. In case the algebraic divergence is taken ($\alpha = 0.33(5)$) a value of $\alpha + 2\beta + \gamma = 2.11(35)$ is obtained, which fulfills the equation better.

The deviation of the hyper-scaling relations from the pure case is obtained by replacing d by $d - \theta$, with the exponent $\theta = 2 - \overline{\eta} + \eta = 1.81(6)$. E.g. the hyper-scaling relation

$$2 - \alpha = \nu(d - \theta) \quad (24)$$

is also fulfilled within error bars ($\nu(d-\theta) = 1.70(30)$), again the case were it is assumed that the "specific heat" diverges faster than logarithmic matches the relation better.

Finally, we turn to the question whether there are two or three independent exponents. In the case of two exponents, the Schwartz-Soffer equation[14]

$$\overline{\gamma} = 2\gamma \quad (25)$$

holds, which is compatible with the result found here. Hence, the two-exponent scenario is supported.

To summarize, all critical exponents of the four-dimensional RFIM were determined independently. All "classical" (hyper-) scaling relations are fulfilled and the two-independent-exponents scenario is supported. The scaling relation proposed in Ref. 21 seems not to be fulfilled. The largest uncertainty in the results presented here is in the value of α, whether $\alpha = 0$ or $\alpha > 0$ and small. To finally decide this question, much larger system sizes must be studied, which are currently out of reach.

Acknowledgments

The author thanks A.P. Young for hosting him at the University of California Santa Cruz, where the work was performed, many helpful discussions and critically reading the manuscript. The work has benefited much from discussions with D. Belanger, R. Kühn, A.A. Middleton, M. Moore and N. Sourlas. The simulations were performed on a Beowulf Cluster at the Institut für Theoretische Physik of the Universität Magdeburg and at the Paderborn Center for Parallel Computing both in Germany. Financial support was obtained from the DFG (Deutsche Forschungsgemeinschaft) under grant Ha 3169/1-1.

* Electronic address: hartmann@lps.ens.fr

[1] D.J. Amit, *Field Theory, The Renormalization Group and Critical Phenomena*, (World Scientific, Singapore 1984)
[2] J. Cardy, *Scaling and Renormalization in Statistical Physics*, (Cambridge University Press 1996)
[3] A.P. Young (ed.), *Spin glasses and random fields*, (World Scientific, Singapore 1998)
[4] S. Fishman and A. Aharony, J. Phys. **C12**, L729 (1979)
[5] J.L. Cardy, Phys. Rev. B **29**, 505 (1984)
[6] D.P. Belanger, in: A.P. Young (ed.), *Spin Glasses and Random Fields*, (World Scientific, Singapore 1998)
[7] A. Aharony, Y. Imry, and S.K. Ma, Phys. Rev. Lett. **37**, 1364 (1976)
[8] A.P. Young, J. Phys. C **10**, L257 (1977)
[9] G. Parisi and N. Sourlas, Phys. Rev. Lett. **43**, 744 (1979)
[10] J. Bricmont and A. Kupiainen, Phys. Rev. Lett. **59**, 1829 (1987)
[11] J. Villain J. Physique **46**, 1843 (1985)
[12] A.J. Bray and M.A. Moore, J. Phys. C **18** L927 (1985)
[13] D.S. Fisher, Phys. Rev. Lett. **56**, 416 (1986)
[14] M. Schwartz and A. Soffer, Phys. Rev. Lett. **55**, 2499 (1985)
[15] M. Schwartz, J. Phys. C **18**, 135 (1985); M. Schwartz and A. Soffer, Phys. Rev. B **33**, 2059 (1986); M. Schwartz, M. Gofman, and T. Nattermann, Physica A **178**, 6 (1991); M. Schwartz, Europhys. Lett. **15**, 777 (1994)
[16] M. Gofman, J. Adler, A. Aharony, A. B. Harris, and M. Schwartz, Phys. Rev. Lett. **71**, 1569 (1993)
[17] H. Rieger, Phys. Rev B **52**, 6659 (1995); See also H. Rieger and A.P. Young, J. Phys. A **26**, 5279 (1993)
[18] A.K. Hartmann and U. Nowak, Eur. Phys. J. B **7**, 105 (1999)
[19] A.K. Hartmann and A.P. Young, Phys. Rev. B **64**, 214419 (2001)
[20] A.A. Middleton and D.S. Fisher, to appear in Phys. Rev. B (2002)
[21] U. Nowak, K.D. Usadel and J. Esser, Physica A **250**, 1 (1998)
[22] A. Aharony, Phys. Rev B **18**, 3318 (1978)
[23] J.C. Anglès d'Auriac, M. Preissmann and A. Seb, J. Math. and Comp. Model. **26**, 1 (1997)
[24] H. Rieger, in: *Advances in Computer Simulation*, Ed. J. Kertesz and I. Kondor, Lecture Notes in Physics **501**, (Springer, Heidelberg 1998)
[25] M.J. Alava, P.M. Duxbury, C. Moukarzel and H. Rieger, in Ed. C. Domb and J.L. Lebowitz, *Phase transitions and Critical Phenomena*, **18**, (Academic press, New York 2001)
[26] A.K. Hartmann and H. Rieger, *Optimization Algorithms in Physics*, (Wiley-VCH, Berlin 2001)
[27] M.R. Swift, A.J. Bray, A. Maritan, M. Cieplak, and J.R. Banavar, Europhys. Lett. **38**, 273 (1997)
[28] M. N. S. Swamy and K. Thulasiraman, *Graphs, Networks and Algorithms*, (Wiley, New York 1991)
[29] J. D. Claiborne, *Mathematical Preliminaries for Computer Networking*, (Wiley, New York 1990)
[30] W. Knödel, *Graphentheoretische Methoden und ihre Anwendung*, (Springer, Berlin 1969)
[31] K. Mehlhorn and St. Näher, *The LEDA Platform of Combinatorial and Geometric Computing*, Cambridge University Press, Cambridge 1999; see also http://www.mpi-sb.mpg.de/LEDA/leda.html.
[32] J.-C. Picard and H. D. Ratliff, Networks **5**, 357 (1975)
[33] J. L. Träff, Eur. J. Oper. Res. 89, 564 (1996)
[34] R. E. Tarjan, *Data Structures and Network Algorithms*, (Society for Industrial and Applied Mathematics, Philadelphia 1983)
[35] A.V. Goldberg and R.E. Tarjan, J. ACM **35**, 921 (1988)
[36] B. Cherkassky and A. Goldberg, Algorithmica **19**, 390 (1997)
[37] A.V. Goldberg, R. Satish, J. ACM, **45**, 783 (1998)
[38] A.A. Middleton, Phys. Rev. Lett. **88**, 017202 (2002)
[39] A.A. Middleton, unpublished (2002)
[40] A.T. Ogielski, Phys. Rev. Lett.**57**, 1251 (1986)
[41] J.-C. Anglès d'Auriac and N. Sourlas, Europhys. Lett. **39**, 473 (1997)
[42] N. Sourlas, Comp. Phys. Comm. **121-122**, 183 (1999)
[43] The RFIM with a delta-distribution of the random fields ($\pm h$) exhibits an exponential ground-state degeneracy.
[44] J.-C. Picard and M. Queyranne, Math. Prog. Study 13, 8 (1980)
[45] A.K. Hartmann, Physica A **248**, 1 (1998)
[46] S. Bastea and P.M. Duxbury, Phys. Rev. E **58**, 4261 (1998)
[47] K. Binder, Z. Phys. B **43**, 119 (1981)
[48] R.N. Bhatt and A.P. Young, Phys. Rev. Lett. **54**, 924 (1985); Phys. Rev. B **37**, 5606 (1988)
[49] W.H. Press, S.A. Teukolsky, W.T. Vetterling and B.P. Flannery, *Numerical Recipes in C*, (Cambridge University Press, Cambridge 1995)
[50] D. P. Belanger, A. R. King, V. Jaccarino and J. L. Cardy, Phys. Rev. B **28**, 2522 (1983); D. P. Belanger and Z. Slanič, J. Magn. and Magn. Mat. **186**, 65 (1998)
[51] V. Privman, P.C. Hohenberg, and A. Aharony, in *Phase Transitions and Critical Phenomena*, Vol. 14, Ed. C. Domb and J.L. Lebowitz, p. 1, (Academic Press, New York 1991)
[52] B. Efron, *The Jackknife, the Bootstrap and Other Resampling Plans*, (SIAM 1982)